

900-979

ANALYSIS OF PARAMETRIC RESONANCES  
OF THE SHUTTLE THERMAL PROTECTION SYSTEM

(NASA-CR-185899) ANALYSIS OF PARAMETRIC  
RESONANCES OF THE SHUTTLE THERMAL PROTECTION  
SYSTEM (JPL) 32 p

N90-70407

unclas

00/16 0234048

LANGLEY RESEARCH CENTER  
LIBRARY NASA  
HAMPTON VIRGINIA

Jet Propulsion Laboratory  
California Institute of Technology

#234048

900-979

ANALYSIS OF PARAMETRIC RESONANCES  
OF THE SHUTTLE THERMAL PROTECTION SYSTEM

February 2, 1981

M. Zak

Jet Propulsion Laboratory  
California Institute of Technology

This work was performed by the Jet Propulsion Laboratory, California Institute of Technology under NASA Contract NAS7-100 in support of the NASA Structures Team.

## Abstract

A mathematical model describing the stable non-linear torsional vibrations of the Space Shuttle tile-strain isolator pad, assembly parametrically induced by normal excitation, is derived. In this treatment the model is represented by a second order non-linear equation with time-dependent coefficients.

To analyze the non-linear vibratory behavior of this system an approximate analytical method of equivalent linearization in combination with the Rayleigh method has been used.

Because of the anisotropic and non-elastic behavior of the strain isolator, an equivalent Young's modular and Poisson's ratio were introduced. These data was derived from a comparison of the analytical solution with experimental data.

The mathematical model so derived allows the evaluation of the vibratory behavior of SIP-tile system under any loading including random excitation.

## Contents

1. Introduction . . . . .	1
2. Conditions for the Loss of Stability of the Strain Isolation System . . . . .	4
3. Governing Equations for Torsional Vibrations . . . . .	7
4. Method of Equivalent Linearization . . . . .	9
5. Conditions of Instability in the Zones of Parametrical Resonance . . . . .	12
6. Identification of the Elastic Modulii . . . . .	16
7. Evaluation of Damping to Suppress Self-Induced Vibrations . . . . .	17
8. Parametric Response to Random Excitations . . . . .	19
9. Conclusions. . . . .	25
References . . . . .	27

## 1. Introduction

This work was motivated by the results of experiments performed by the NASA Langley Research Center. These experiments exhibited torsional Strain Isolation Pad (SIP) tile vibrations and failure induced by sinusoidal excitations applied at the base: when excited sinusoidally in the normal direction in the range of 60 to 90 Hertz at a level above 15g, a fundamentally nonlinear dynamic instability occurred in which in-plane motions exceeding 2.5mm were observed. These in-plane torsional responses occurred at a frequency of exactly one half the excitation frequency.

Three basic conclusions follow from these results.

1. Because torsional in-plane vibrations are induced by out-of-plane disturbances, the phenomenon is due to a mechanism of instability.
2. The mechanism of instability is associated with a parametric resonance because in-plane responses occurred at a frequency of exactly one-half of the excitation frequency.
3. The phenomenon is strongly nonlinear because the initial instability in the area of small deformations is replaced by stable self-induced vibrations of a finite amplitude.

In order to better understand the non-linear vibratory nature of this system and in order to predict its behavior under certain loads which cannot be modeled in the course of experiments, a mathematical model had to be developed.

The simplest mathematical model describing a parametrical resonance is given in the form of an ordinary linear differential equation of the second order with a time-dependent coefficient:

$$\ddot{\psi} + (k - g_0 \sin \omega t) \psi = 0 \quad (1)$$

where  $\psi$  is the torsional angle

$\rho_0$  is the amplitude of normal excitation

$\omega$  is the frequency of normal excitation

$k = \text{Const}$  is the torsional stiffness.

This equation is called the Mathieu equation. Its solutions are expressed in the form of special (Mathieu) functions.

As is proven in the theory of Mathieu equations there are some areas of instability of the solutions if the eigenfrequency  $\Omega = \sqrt{k}$  is close enough to one-half the exciting frequency  $\omega$  i.e.

$$\omega = 2\sqrt{k} \quad (2)$$

The solutions in this area of instability is presented in the following form:

$$\psi = C_1 e^{\mu t} \varphi_1(t) + C_2 e^{-\mu t} \varphi_2(t) \quad (3)$$

where  $\varphi_1(t), \varphi_2(t)$  are some periodical functions,  $C_1, C_2$  are constants of integration

and

$$\mu^2 > 0 \quad (4)$$

It is seen that irrespective of the sign of  $\mu$ , one of the terms in Eq. (3) will grow without limit if  $t \rightarrow \infty$ . This means that a parametric resonance is a typical case of instability which can be generated by infinitesimal random disturbances.

There are several differences between parametric and forced resonances:

- 1) A forced resonance is associated with a stable system and can occur even without initial (disturbances while a parametrical resonance is a result

of instability of the initial state and can occur only due to initial disturbances.

- 2) In the response of a forced resonance the amplitude of vibration grows linearly with respect to time, while in the response of a parametrical resonance the amplitude grows exponentially. That is why a forced resonance can be limited by linear damping:

$$t e^{-\varepsilon t} \rightarrow 0 \text{ if } t \rightarrow \infty, \varepsilon > 0 \quad (5)$$

while a parametric resonance can be depressed only if the linear damping exceeds some particular value:

$$e^{(\mu - \varepsilon)t} \rightarrow 0, \text{ if } t \rightarrow \infty, \varepsilon > \mu \quad (6)$$

- 3) A forced resonance occurs at discrete frequencies while a parametrical resonance covers a continuum of frequencies in the area of instability.

The degeneration of a parametric resonance into stable self-induced vibrations with finite amplitude is typical nonlinear phenomenon due to the increase of the stiffness with an increase of the amplitude of vibration. In the simplest form this nonlinearity can be introduced by an additional term in Eq. (1):

$$\ddot{\psi} + (k - q_0 \sin \omega t) \psi + k_2 \psi^3 = 0, \quad k_2 > 0 \quad (7)$$

In this report, the nonlinear second order equation of motion of the form of Eq. (7) governing the nonlinear torsional SIP-tile parametrical resonance is derived by exploring the method of equivalent linearization in a combination with the Rayleigh method, the area of instability and maximum amplitude of self-induced vibrations are defined in closed form.

## 2. Conditions for the Loss of Stability for the Strain Isolation System

The transition from normal to torsional displacements can be explained by the loss of stability of the SIP as a result of compression. The compression of the SIP during normal excitation is generated by the inertia forces:

$$\rho \approx \frac{m\alpha}{B^2} \quad (8)$$

where  $\rho$  is the average pressure in the SIP

$\alpha$  is the normal acceleration

$B^2$  is the area of the SIP

$m$  is the mass of the SIP-tile system.

As shown in the non-linear theory of elasticity [1], the loss of stability is associated with failure of hyperbolicity of the governing equations. From the mathematical point of view it corresponds to the appearance of imaginary characteristic speeds of wave propagation. From the mechanical point of view this leads to appearance of local maxima in potential energy as a function of strains in the directions where the characteristic speed is imaginary.

There are two types of characteristic speeds in the compressed SIP:

$$\lambda_1 = \pm \sqrt{\frac{-\rho + E}{\rho}} \quad (9)$$

$$\lambda_2 = \pm \sqrt{\frac{-\rho + G}{\rho}} \quad (10)$$

where  $\lambda_1$  is the characteristic speed of longitudinal waves

$\lambda_2$  is the characteristic speed of transverse waves

$E, G$  are the Young's and shear moduli of SIP

$\rho$  is the density of SIP



For the classical structural materials like steel in the domain of elasticity:

$$E, G \gg \rho \quad (11)$$

i.e. both of the characteristic speeds  $\lambda_1, \lambda_2$  are real and the instability described above does not occur. However, for soft materials like rubber, textile materials, etc, the shear modulus  $G$  can be sizable compared to the pressure in the domain of elasticity

$$\rho \sim G \quad (12)$$

The material of SIP is not only soft, but in addition it possesses a filament type of microstructure which reduces significantly the through-thickness shear modulus.

Using Eq. (8) the pressure can be evaluated as:

$$\rho \sim 200 \frac{\text{kg}}{\text{M}^2} \quad (13)$$

if

$$m = 0.319 \text{ kg}, \quad \alpha = 15.5 \text{ g} \frac{\text{M}}{\text{sek}^2}, \quad \beta = 0.152 \text{ M}$$

i.e. the loss of stability of the microstructure of the SIP occurs if

$$G_{t \text{ t t}}^0 \sim 200 \frac{\text{kg}}{\text{M}^2} = 0.23 \text{ psi} \quad (14)$$

where  $G_{t \text{ t t}}^0$  is the through the thickness shear modulus at the instance of the loss of stability.

In the course of this instability the initially vertical filaments become curved or sloped (Fig. 1)

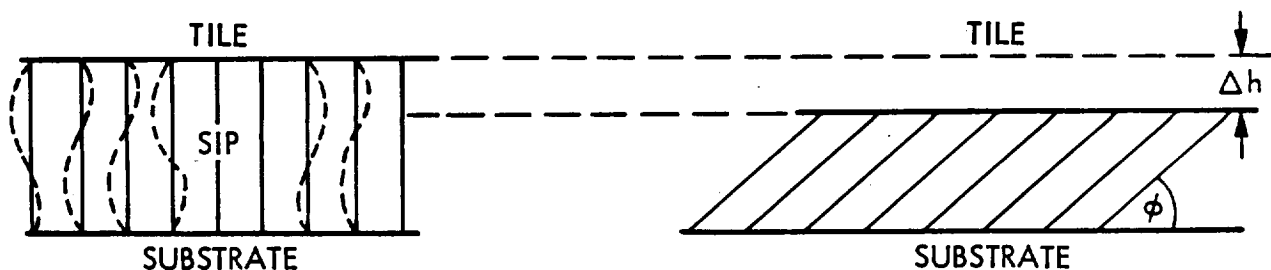


Fig. 1

In other words, the compression of the SIP occurs due to the sloping of its vertical filaments rather than by their contraction.

Obviously, the effective through the thickness shear modulus  $G_{ttt}$  will be increasing with an increase in the filament slope, i.e.

$$G_{ttt} > G_{ttt}^0 \quad (15)$$

and this will provide the stability of a new state of the SIP;

$$G_{ttt} > \rho \quad (16)$$

The relationship between the compression  $\varepsilon$  and the slope angle  $\varphi$  follows from geometry:

$$|\varepsilon| = (1 - \cos \varphi) \approx \frac{\varphi^2}{2} \quad (17)$$

and

$$\varepsilon = \frac{\Delta h}{h} \quad (18)$$

where  $h$  is the thickness of the SIP.

Clearly, this dependence holds only for compression, but not for a tension when the thickness  $h$  is increasing ( $\Delta h > 0$ ).

Now in-plane vibrations of the SIP can be presented in the simplest forms:

1. In-plane shear vibrations (Fig. 2).

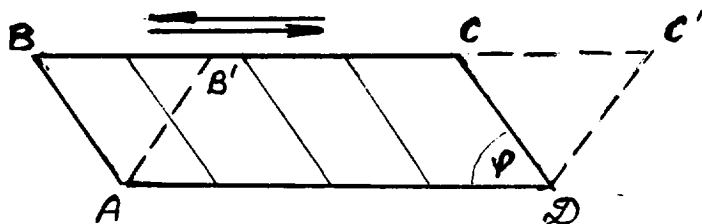


Fig. 2

where ABCD (or AB'C'D) is a vertical SIP cross-section during deformation.

## 2. In-plane torsional vibrations (Fig. 3)

Here ABCD (or AB'CD) is one-half of a vertical SIP cross-section before deformation. For outside filaments the compression is carried out only by torsion while for inside filaments it is carried out mostly by contraction. For instance, for the filament AB the decrease of the SIP thickness CC' is due to the torsion but for the central filament CD - is due to contraction.

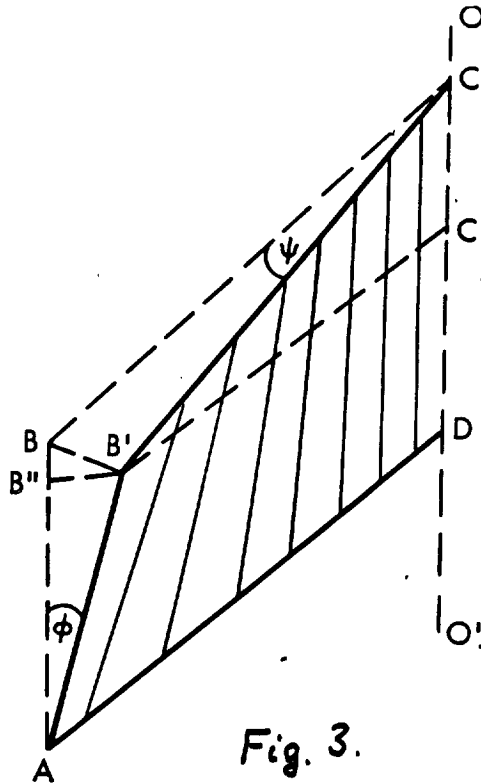


Fig. 3.

The angle of torsion  $\psi$  is related to the slope angle  $\phi$  by the relationship

$$\psi = \frac{b}{2h} \phi \quad (19)$$

where  $b$  is the size of the square tile.

## 3. Governing Equation for Torsional Vibration

In this section attention will be paid to in-plane torsional vibrations although the results can equally be applied to in-plane shear vibrations.

The potential energy of a compressed SIP can be presented as a sum of the potential energy  $\Pi_1$  of contraction of filaments and the potential energy  $\Pi_2$  of torsion that is

$$\Pi_1 = \frac{E_{ttt} \varepsilon^2}{2} b^2 h = \frac{E_{ttt} b^2 h}{2} \frac{\varphi^4}{4} \quad (20)$$

$$\Pi_2 = \frac{0.14 b^4}{2h} G_{ttt} \frac{\varphi^2}{2} \quad (21)$$

where  $E_{ttt}$  is the through the thickness Young's modulus of the SIP.

The virtual work of the external (normal to the substrate) forces is given by the expression:

$$\delta A_e = Q \delta \Delta h = Q h \Delta \varepsilon = Q h \delta \left( \frac{\varphi^2}{2} \right) = Q h \varphi \delta \varphi \quad (22)$$

The virtual work of the torsional inertia forces can be expressed in the following form:

$$\delta A_i = - \frac{m b^2}{6} \ddot{\varphi} \delta \varphi \quad (23)$$

Ignoring the inertia forces due to the contraction of the filaments and using the principle of virtual work:

$$-\delta \Pi_1 - \delta \Pi_2 + \delta A_e + \delta A_i = 0$$

then,

$$\frac{m b^2}{6} \ddot{\varphi} + \frac{0.14 b^4}{h} G_{ttt} \varphi + \frac{b^6}{32 h^3} E_{ttt} \varphi^3 = Q \frac{b^2}{2h} \varphi \quad (24)$$

or

$$\ddot{\psi} + (k_1 - q_0 \sin \omega t) \psi + k_2 \psi^3 = 0 \quad (25)$$

where

$$k_1 = \frac{0.84 B^2}{mh} G_{ttt} \quad (26)$$

$$k_2 = \frac{3 B^4}{16 m h^3} E_{ttt} \quad (27)$$

$$q_0 = \frac{3 Q_0}{mh} \quad (28)$$

while the external force  $Q$  is taken in its simplest form as

$$Q = Q_0 \sin \omega t \quad (29)$$

It is seen that Eq. (25) is identical to Eq. (7) previously discussed.

#### 4. Method of Equivalent Linearization

Eq. (25) is nonlinear because of the last term  $k_2 \psi^3$ . Its analytical investigation cannot be performed without some approximations. Because the main reason for such an investigation is analysis of self-induced vibrations which in the first approximation can be considered as harmonic vibrations, the method of equivalent linearization is applicable.

It has been shown [2] that this method is very effective for the analysis of self-induced vibrations which are governed by even more complicated differential equations than is represented by Eq. (25).

$$G(\omega t) \ddot{\psi} + P(\omega t) \dot{\psi} + k(\omega t) \psi + q(\psi, \dot{\psi}) = Q(\omega t) \quad (30)$$

The basic idea of this method is given below.

Assuming that Eq. 30 possesses in the zone of the parametric resonance a periodical solution which is close to being harmonic and can be presented in the form:

$$\psi^0 = A_0 + A \cos \omega t + B \sin \omega t = A_0 + C \sin \theta \quad (31)$$

where

$$C = \sqrt{A^2 + B^2}, \quad \frac{A}{C} = \sin \alpha, \quad \frac{B}{C} = \cos \alpha, \quad \theta = \omega t + \alpha \quad (32)$$

the non-linear function  $\varphi(\psi^0, \dot{\psi}^0)$  becomes periodical too:

$$\varphi(\psi^0, \dot{\psi}^0) = \varphi_0 + \varphi' \cos \theta + \varphi'' \sin \theta + (\delta) \quad (33)$$

where  $(\delta)$  presents the higher order harmonics in Fourier series and

$$\psi^0 = \frac{1}{2\pi} \int_0^{2\pi} \varphi(\psi^0, \dot{\psi}^0) d\theta \quad (34)$$

$$\psi' = \frac{1}{\pi} \int_0^{2\pi} \varphi(\psi^0, \dot{\psi}^0) d\theta \quad (35)$$

Consider an auxiliary linear differential equation

$$G(\omega t) \ddot{\psi} + [P(\omega t) + \Delta p] \dot{\psi} + [k(\omega t) + \Delta k] \psi + \Delta E = \theta(\omega t) \quad (36)$$

where  $\Delta p, \Delta k, \Delta E$  are unknowns which do not depend on time.

These unknowns can be defined from the requirement that at  $\psi = \psi^0$  the following equality must hold:

$$\begin{aligned} & [P(\omega t) + \Delta p] \dot{\psi}^0 + [k(\omega t) + \Delta k] \psi^0 + \Delta E = \\ & = p(\omega t) \dot{\psi}^0 + k(\omega t) \psi^0 + \varphi_0 + \varphi' \cos \theta + \varphi'' \sin \theta \quad (37) \end{aligned}$$

It is seen that condition (37) makes Eqs. (30) and (37) equivalent within the frame work of the approximations stated before.

Substituting Eq. (33) in Eq. (37) and equaling the coefficients at "sin", "cos" and free terms leads to the following expressions for the coefficients of the equivalent linearization  $\Delta K, \Delta p, \Delta E$ :

$$\Delta k(A_0, C) = \frac{\varphi''}{C} \quad (38)$$

$$\Delta p(A_0, C) = \frac{\varphi'}{\omega C} \quad (39)$$

$$\Delta E = \varphi^0(A_0, C) - A_0 \Delta k(A_0, C) \quad (40)$$

For the particular case when Eq. (30) is degenerated into Eq. (25) the Equations (34), (35), (38)-(40) are simplified:

$$\varphi^0 = \frac{k_2}{2\pi} \int_0^{2\pi} (A_0 + C \sin \theta)^3 d\theta = k_2 A_0 (A_0^2 + \frac{3}{2} C^2) \quad (41)$$

$$\varphi' = \frac{k_2}{\pi} \int_0^{2\pi} (C \sin \theta)^3 \cos \theta d\theta = 0 \quad (42)$$

$$\varphi'' = \frac{k_2}{\pi} \int_0^{2\pi} (C \sin \theta)^3 \sin \theta d\theta = \frac{3}{4} k_2 C \quad (43)$$

$$\Delta k = \frac{3}{4} k_2 C^2 \quad (44)$$

$$\Delta E = k_2 A_0 (A_0^2 + \frac{3}{4} C^2) \quad (45)$$

Now the original non-linear Eq. (25) is replaced by an equivalent linear differential equation:

$$\ddot{\psi} + (k_1 + \frac{3}{4} k_2 C^2 - q_0 \sin \omega t) \psi + k_2 A_0 (A_0^2 + \frac{3}{4} C^2) = 0 \quad (46)$$

In contrast to the originally linear equation (1) this linearized equation possesses a very important property: its stiffness-coefficient depends on the amplitude of vibrations which is unknown so that a formal solution must be considered as an implicit equation with respect to this unknown.

## 5. Conditions of Instability on the Zones of Parametric Resonance

The boundaries of parametric instability in the solution of Eq. (46) can be found by applying the Rayleigh method. The basic idea of this method is as follows: The boundary of dynamic instability separates the zone of damped vibrational response from the zone of divergent vibrational response. That is why at the boundary of instability the vibrational response can be considered as steady and sought in the form of harmonical vibration.

The method will be illustrated in the solution of Eq. (30) using the following Fourier expansions:

$$G(\omega t) = G_0 + \sum_{i=1}^{\infty} G_i \cos i\omega t \quad (47)$$

$$k(\omega t) = k_0 + \sum_{i=1}^{\infty} (K_i^c \cos i\omega t + K_i^s \sin i\omega t) \quad (48)$$

As was discussed before, the main parametric resonance occurs if the eigen-frequency is close to one-half the excitation frequency, i.e.

$$i\omega \approx 2 \sqrt{\frac{K_0}{G_0}} \quad (49)$$

where  $i = 1, 2, \dots$  etc.

that is

$$\omega = \frac{1}{j} \sqrt{\frac{K_0}{G_0}}, \quad j = \frac{1}{2}, 1, \frac{3}{2}, 2, \frac{5}{2} \text{ etc} \quad (50)$$

Then for each  $j$  the corresponding solution can be sought in the form:

$$y = A_0 + A_j \cos j\omega t + B_j \sin j\omega t \quad (51)$$



Substituting (51) into Eq. (30), and setting to zero the coefficients of the ~~sines, cosines and~~ free terms and ignoring terms of higher order:

$$A_0 k_0 + \mathcal{D}_j A_j + \frac{1}{2} k_j^s B_j = 0 \quad (52)$$

$$A_0 k_j^c + (k_0 - j^2 \omega^2 G_0 + \mathcal{D}_{2j}) A_j + \frac{1}{2} k_{2j}^s B_j \quad (53)$$

$$A_0 k_j^s + \frac{1}{2} k_{2j}^s A_j + (k_0 - j^2 \omega^2 G_0 - \mathcal{D}_{2j}) B_j = 0 \quad (54)$$

where

$$\mathcal{D}_j = \frac{1}{2} (k_j^c - j^2 \omega^2 G_j) \quad (55)$$

$$\mathcal{D}_{2j} = \frac{1}{2} (k_{2j}^c - j \omega^2 G_{2j}) \quad (56)$$

The conditions of the existence of a non-zero solution corresponds to a zero determinant:

$$\Gamma(\omega^2) = \frac{1}{k_0} \begin{vmatrix} k_0 & \mathcal{D}_j & \frac{1}{2} k_j^s \\ k_j^c & k_0 - j^2 \omega^2 G_0 + \mathcal{D}_{2j} & \frac{1}{2} k_{2j}^s \\ k_j^s & \frac{1}{2} k_{2j}^s & k_0 - j \omega^2 G_0 - \mathcal{D}_{2j} \end{vmatrix} \quad (57)$$

This characteristic equation defines critical frequencies  $\omega$  for each  $j$ .

Clearly, two different situations are possible.

1.  $\Gamma(\omega^2) > 0$  i.e. there are no real frequencies. This means, that a parametrical resonance is impossible at the corresponding  $j$ .

2. There are two positive roots  $\omega_1, \omega_2$ . Then the zone of frequencies  $\omega$

$$\omega_1 \leq \omega \leq \omega_2 \quad (58)$$

is unstable, and  $\Gamma > 0$  corresponds to stability, while  $\Gamma < 0$  corresponds to instability.

For the main resonance  $j = \frac{1}{2}$  and  $G = G_0, k^c = 0$  the characteristic equation is simplified

$$\Gamma_2 Z^4 + \Gamma_1 Z^2 + \Gamma_0 = 0 \quad (59)$$

where  $Z^2 = \frac{\omega^2}{k_0}$

$$\Gamma_0 = 1 - \frac{1}{4} \left( \frac{k_1^s}{k_0} \right)^2, \quad \Gamma_1 = -\frac{1}{2}, \quad \Gamma_2 = \frac{1}{16}$$

For the particular case of Eq. (46)

$$k_0 = k_1 + \frac{3}{4} k_2 C^2, \quad k_1^s = -q_0 \quad (60)$$

where  $C$  is the amplitude of vibrations.

Hence:

$$\omega^2 = 4(k_1 + 3k_2 C^2) \pm 2q_0 \quad (61)$$

Thus, the main resonance initially (for small amplitudes  $C$ ) occurs not only at the frequency

$$\omega = 2k_1 \quad (62)$$

but also within the zone:

$$\sqrt{4k_1 - 2q_0} \leq \omega \leq \sqrt{4k_1 + 2q_0} \quad (63)$$

which depends on the external load.

The unstable zone is drawn in the Figure 4

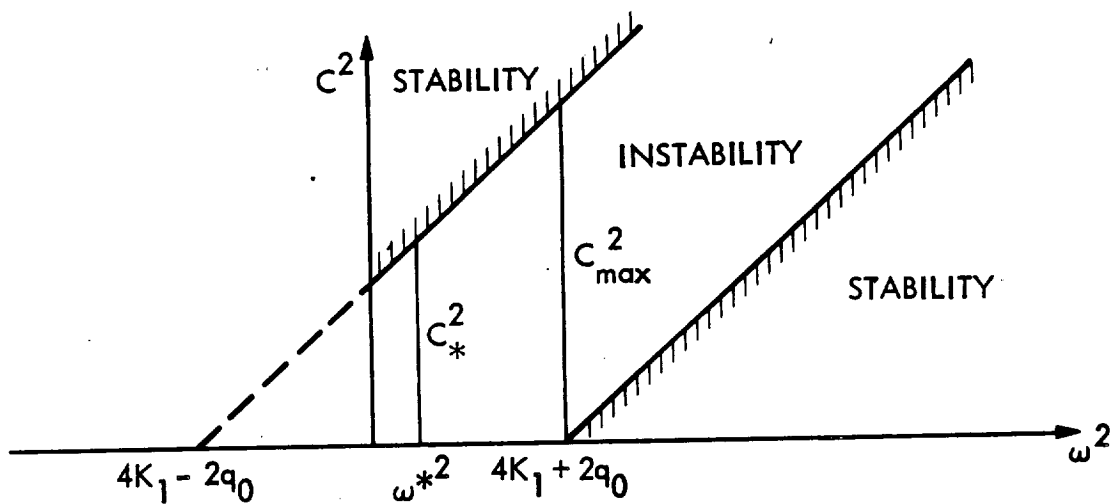


Fig. 4

It follows from this figure, that maximum amplitude of vibration is given by:

$$C_{max} = \sqrt{\frac{4q_0}{3k_2}} = \frac{h}{b^2} \sqrt{\frac{4 \cdot 16Q_0}{3E_{ttt}}} \quad (64)$$

when

$$\omega = \omega_{max} = \sqrt{4k_1 + 2q_0} \quad (65)$$

Indeed, if for some reason

$$C > C_{max} \quad (66)$$

then the response becomes stable and the amplitude will start decreasing up to  $C_{max}$ . Clearly, such a mechanism leads to self-induced vibrations with the amplitude  $C_{max}$

## 6. Identification of the Elastic Modulii

Exploring the experimental results according to which

$$b = 0.152 \text{ m}$$

$$h = 0.004 \text{ m}$$

$$m = 0.319 \text{ kg}$$

$$\omega_{max} = 80 \text{ Hz}$$

$$Q/m = 15 \text{ g}$$

$$C_{max} = 0.03$$

the equivalent modulii  $E_{ttt}$ ,  $G_{ttt}$  are defined by the formulas (64), (65):

$$E_{ttt} = 7680 \frac{\text{kg}}{\text{m}^2} = 9.12 \text{ psi} \quad (67)$$

$$G_{ttt} = 57 \frac{\text{kg}}{\text{m}^2} = 0.06 \text{ psi} \quad (68)$$

Such a low value of the equivalent modulus  $G_{ttt}$  confirms the assumption that the mechanism of torsion is associated with the instability of the shape of the SIP filaments.

# 7. Evaluation of Damping to Suppress Self-Induced Vibrations.

For the evaluation of the damping to suppress self-induced vibrations the energy method can be applied. Exploring Eq. (68) and assuming the existence of damping (due to the pumping of air by the SIP or due to viscous additions) the equation of motion can be written:

$$\ddot{\psi} + \beta \dot{\psi} + (k_1 + \frac{3}{4} k_2 + q_0 \sin \omega t) \psi = 0 \quad (69)$$

where  $\beta$  is the damping coefficient.

The comparison of the work done during the period of one cycle by the existing force:

$$\Delta E_F = q_0 \psi_0^2 \Omega^2 \int_0^{2\pi/\Omega} \sin \Omega t \cos \Omega t \sin \omega t dt = \frac{\pi}{2} q_0 \psi_0^2 (\omega = 2\Omega)$$

and the dissipating force

$$\Delta E = \beta \psi_0^2 \Omega^2 \int_0^{2\pi/\Omega} \sin^2 \Omega t dt = \frac{\beta \psi_0^2 \omega}{2} (\omega = 2\Omega)$$

leads to the following evaluation:

$$\Delta E > \Delta E_F$$

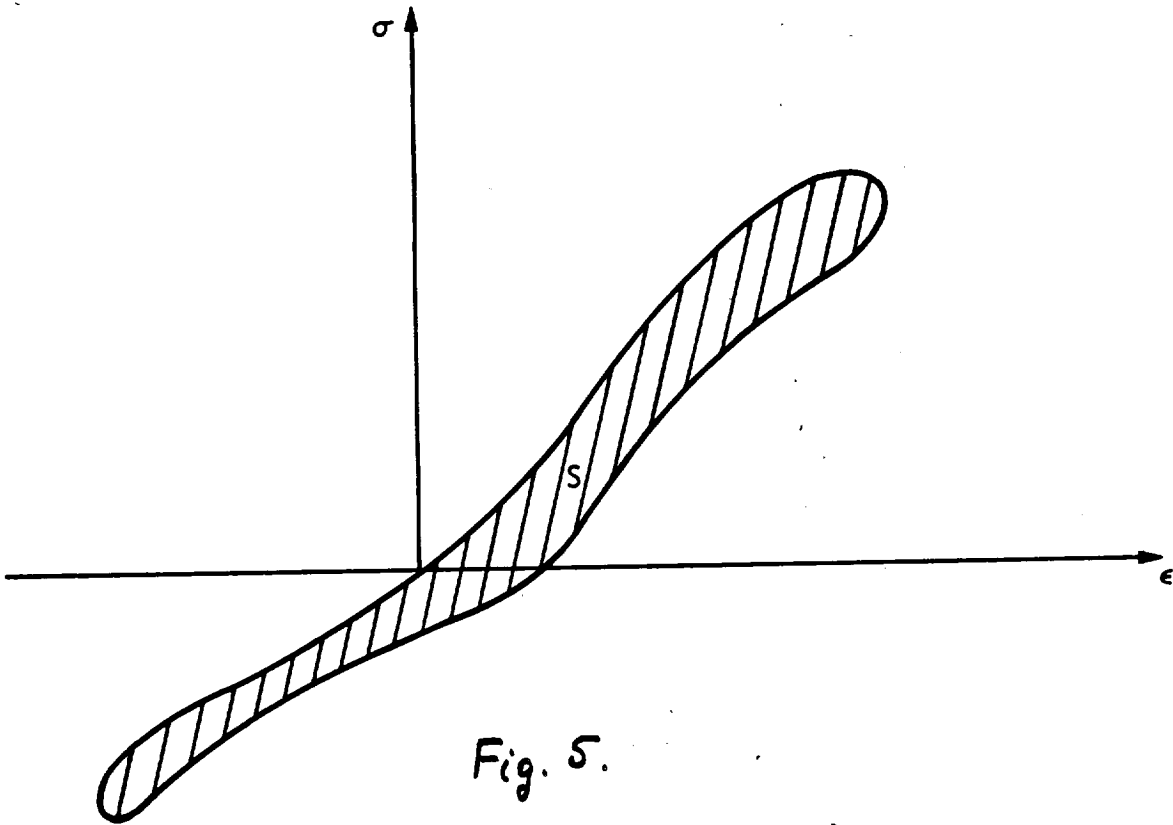
if

$$\beta > \frac{\pi q_0}{\omega} \quad (70)$$

As shown in Ref. 2 the damping coefficient can be subdivided in two parts:

$$\beta = \beta_0 + \frac{6Sh}{\pi m \psi_0^2 \omega} \quad (71)$$

where  $\beta_0$  is the coefficient of linear damping, while the second term in Eq. (71) corresponds to a non-linear damping due to the loop of hysteresis in the SIP stress-strain characteristic ( $S$  is the area of this loop), Figure 5.



Thus it follows from (70) and (71):

$$\beta_0 + \frac{6Sh}{\pi m \varphi_0^2 \omega} > \frac{\pi \varphi_0}{\omega} \quad (72)$$

It is seen that the linear term loses its effectiveness for low frequencies, while the nonlinear term loses its effectiveness for high amplitudes. That is why both of the terms in (72) are important.

But it follows from (63) that a parametric resonance for a selected sample of a SIP-tile assembly can occur at any frequency up to  $80 \text{ Hz}$ . Hence, for a conservative evaluation instead of (72) it can be written:

$$S > \frac{\pi^2 m \varphi_0^2 \varphi_0}{6h} = \frac{\pi^2 C_{\max}^2 \varphi_0}{h^2} \quad (73)$$

For the load given in the experiment mentioned above

$$S > 1180 \frac{kg}{m^2} = 1.4 psi \quad (74)$$

# 8. Parametrical response to random excitations.

Random loads are usually given in the form of the spectral density:

$$\varphi = \varphi(\omega) \quad (75)$$

which is proportional to the mean power of the process in the interval of frequencies from  $\omega$  to  $\omega + d\omega$ .

In this interval the force can be approximately presented in the form:

$$F = \sqrt{\frac{2}{\pi} \varphi(\omega)} \sin \omega t \quad (76)$$

In terms of Eq. (46) for the main resonance, i.e. for

$$j = \frac{1}{2}, \quad A_0 = 0 \quad (77)$$

this force is given in the form

$$q = q_0(\omega) \sin \omega t \quad (78)$$

so that instead of Eq. (46) the governing equation is the following:

$$\ddot{\psi} + [k_1 + \frac{3}{4} k_2 C^2 - q_0(\omega) \sin \omega t] \psi = 0 \quad (79)$$

The dependence of the amplitude  $q_0$  on the frequency  $\omega$  leads to the transcendental characteristic equation instead of (59)

$$\frac{1}{16} Z^4 - \frac{1}{2} Z^2 + 1 - \frac{1}{4} \left[ \frac{q_0 (k_0 Z^2)}{k_0} \right]^2 = 0 \quad (80)$$

In order to solve this equation analytically the function  $q_0(\omega)$  will be approximated piece-wise in the form

$$q_0^2 = \alpha \omega^2 + \beta, \quad \omega_1 \leq \omega \leq \omega_2 \quad (81)$$

where the coefficients  $\alpha, \beta$  are constants within the corresponding interval.

Then for each interval the characteristic equation (80) is written in the simplified algebraic form:

$$Z^4 - (8 + 16\alpha^*) Z^2 + 16(\beta^* + 1) = 0 \quad (82)$$

where

$$\alpha^* = \frac{\alpha}{k_0}, \quad \beta^* = \frac{\beta}{k_0^2}$$

Now if the roots of this equation:

$$Z^2 = (4 + 8\alpha^*) \pm \sqrt{(4 + 8\alpha^*)^2 - 16(\beta^* + 1)} \quad (83)$$

i. e.

$$\omega = \pm \sqrt{k_0 \left[ (4 + 8\alpha^*) \pm \sqrt{(4 + 8\alpha^*)^2 - 16(\beta^* + 1)} \right]} \quad (84)$$

are outside of the corresponding interval (81), then a parametrical resonance cannot occur.





D-26

# AFT FUS FLOOR CRITERIA DEVELOPMENT

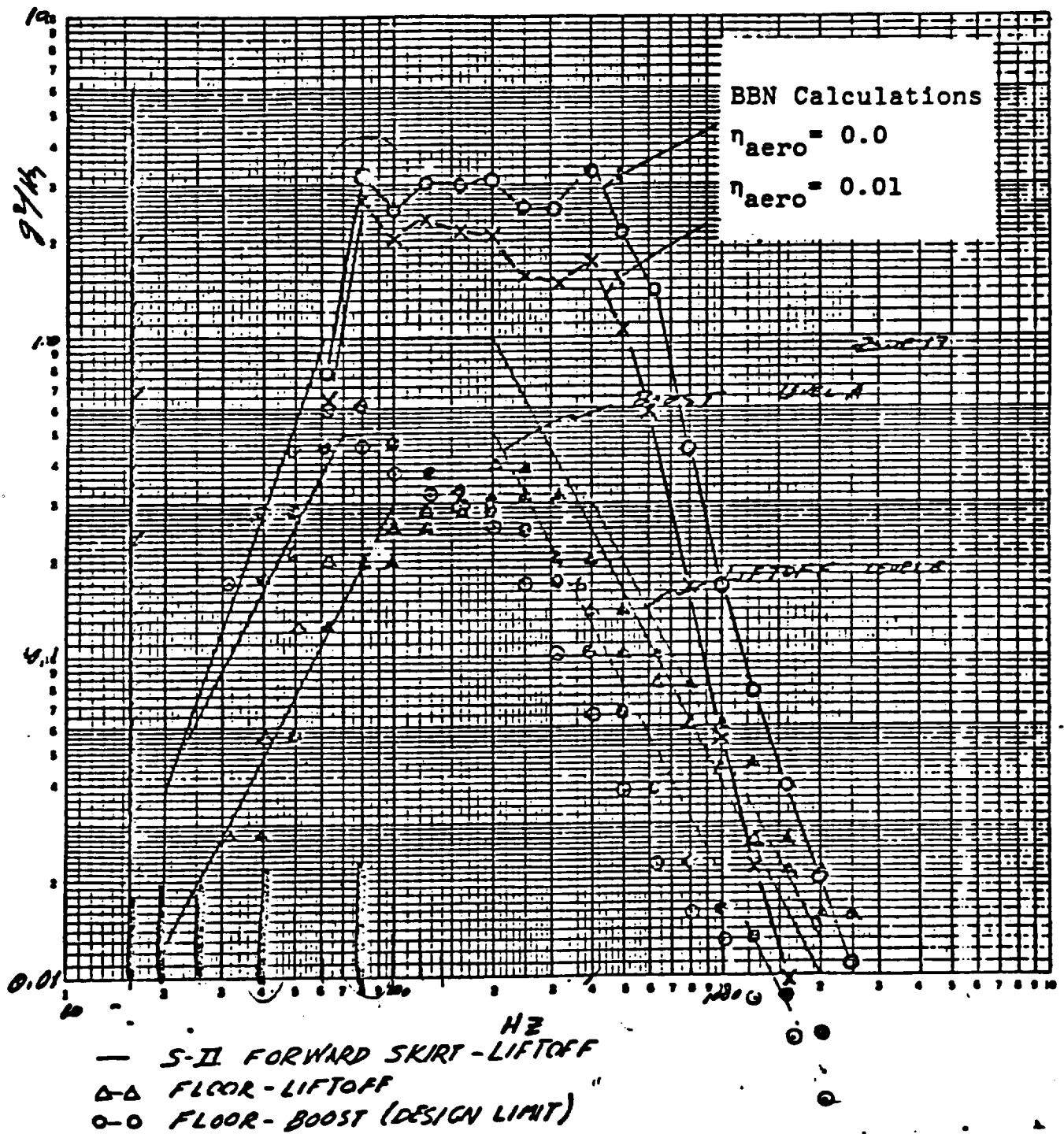


Figure 6 : Aft fuselage floor acceleration spectral density  
for aerodynamic excitation

The parametrical resonance is possible only if even one of the characteristic roots occurs within the interval (81).

This theory will be applied to the random loads given in Figure 6. The curve can be subdivided in three zones:

$$\text{Zone 1: } 0 \leq \omega \leq 500 \frac{1}{\text{sec}} \quad (85)$$

$$\text{Zone 2: } 500 \frac{1}{\text{sec}} \leq \omega \leq 2500 \frac{1}{\text{sec}} \quad (86)$$

$$\text{Zone 3: } 2500 \frac{1}{\text{sec}} \leq \omega \leq 18850 \frac{1}{\text{sec}} \quad (87)$$

The calculation of the coefficient  $\alpha, \beta$  gives:

$$\alpha_1 = 675 \frac{1}{\text{sec}^2}, \quad \beta_1 = -9 \cdot 10^7 \frac{1}{\text{sec}^4} \quad (88)$$

$$\alpha_2 = 62 \frac{1}{\text{sec}^2}, \quad \beta_2 = 9 \cdot 10^7 \frac{1}{\text{sec}^4} \quad (89)$$

$$\alpha_3 = -170 \frac{1}{\text{sec}^2}, \quad \beta_3 = 1.6 \cdot 10^9 \frac{1}{\text{sec}^4} \quad (90)$$

Hence for  $\alpha^*, \beta^*$  at zero amplitude ( $C=0$ ):

$$\alpha_1^* = 0.08, \quad \beta_1^* = -1.2 \quad (91)$$

$$\alpha_2^* = 0.007, \quad \beta_2^* = 1.2 \quad (92)$$

$$\alpha_3^* = -0.02, \quad \beta_3^* = 22 \quad (93)$$

Substituting (91) through (93) into Eq. (86) shows that for the frequency intervals (86), (87) the characteristic roots are imaginary, while for the interval (85) there are two real roots corresponding to the following critical frequencies for zero amplitudes:

$$\omega_1 \approx 0, \quad \omega_2 = 285 \frac{1}{\text{sec}} \approx 45 \text{ Hz} \quad (94)$$

which means that a parametrical resonance occurs in the first interval of frequencies (85)

Now following the procedure performed in the item 5 the analog of Eq. (61) is given by:

$$\omega^2 = \left(k_1 + \frac{3}{4} k_2 c^2\right) \left\{ \left(4 + \frac{0.64}{1 + \frac{3}{4} \frac{k_2}{k_1} c^2}\right) \pm \sqrt{\left(4 + \frac{0.64}{1 + \frac{3}{4} \frac{k_2}{k_1} c^2}\right)^2 - 16 \left[1 - \frac{1.2}{\left(1 + \frac{3}{4} \frac{k_2}{k_1} c^2\right)^2}\right]} \right\} = f(c^2) \quad (95)$$

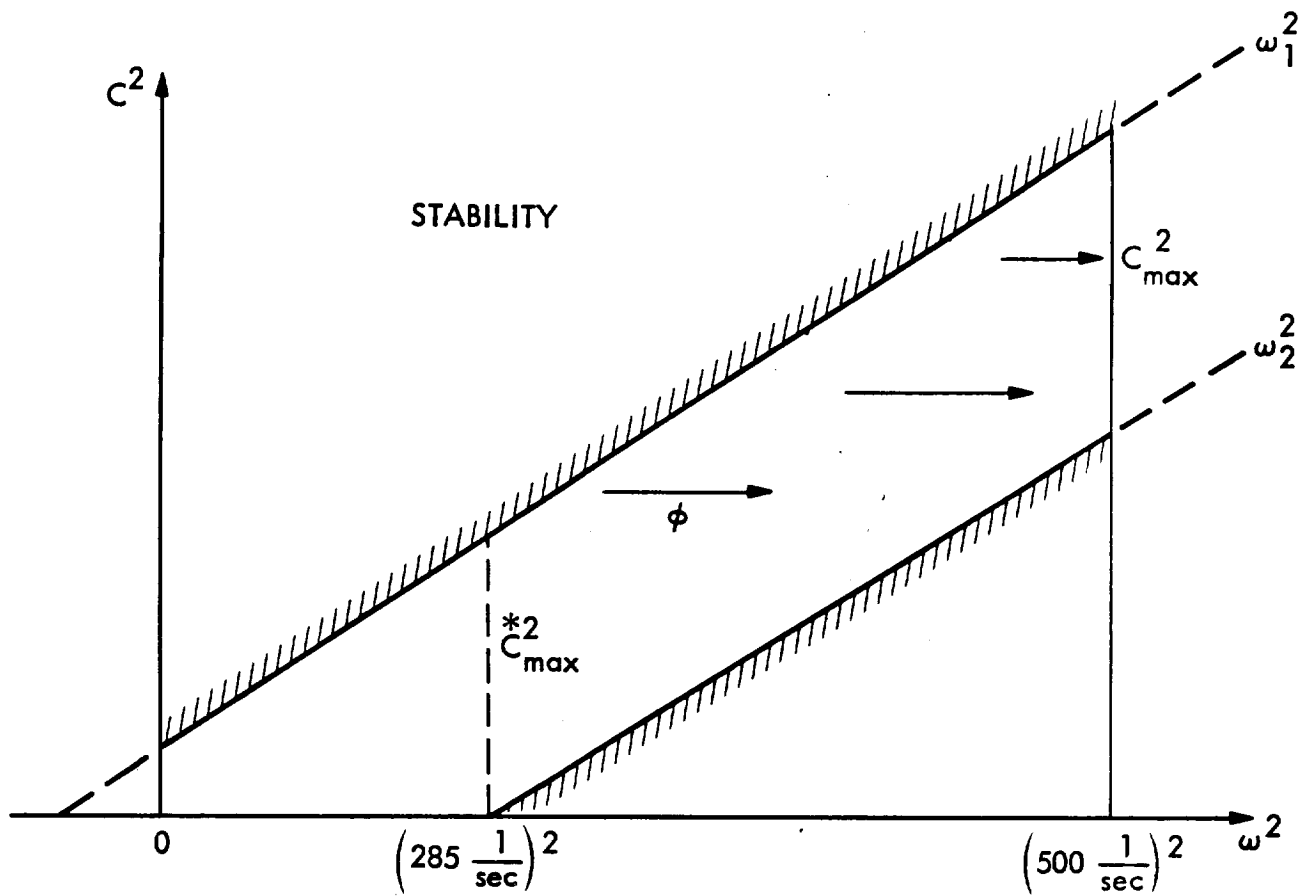
or approximately:

$$\omega_{1,2}^2 = 4 \left(k_1 + \frac{3}{4} k_2 c^2\right) \pm 4.4 k_1 \quad (96)$$

The boundaries of instability

$$\omega_1^2 = f_1(c^2), \quad \omega_2^2 = f_2(c^2) \quad (97)$$

are plotted in Figure 7 which is similar to the Figure 4



where

$$f_1 = 4(k_1 + \frac{3}{4}k_2 c^2) - 4.4k_1 \quad (98)$$

$$f_2 = 4(k_1 + \frac{3}{4}k_2 c^2) + 4.4k_1 \quad (99)$$

or exploring the data from the item 6:

$$\frac{\omega_1^2}{k_1} = 43500 c^2 - 0.4 \quad (100)$$

$$\frac{\omega_2^2}{k_1} = 43500 c^2 + 8.4 \quad (101)$$

The amplitude at the frequency  $\omega_2 = 45 \text{ Hz}$  is

$$C_{\max}^* = 0.015 \quad (102)$$

i.e. one-half the maximum amplitude observed in the experiment.

However, it is important to emphasize that this maximum amplitude corresponds only to those vibrations which are initially unstable, i.e. when the instability appears at  $C \rightarrow 0$ . For single-harmonic excitation such a method for the determination of the maximum amplitude is reasonable because the probability of large initial torsional disturbances can be ignored. In contrast to this, for random excitations containing all the frequencies, the probability of large initial torsional disturbances cannot be ignored because these disturbances can be parametrically induced by lower frequencies and then shifted towards the higher frequencies (Fig. 7).

That is why for random excitations, self-induced vibrations with frequencies higher than 45 Hz are also possible and the maximum amplitude will correspond to 80 Hz but not 45 Hz:

$$C_{\max} = 0.026 \quad (103)$$

This amplitude is comparable with the amplitude observed in the experiment ( $C = 0.03$ ) accompanied with the failure of the SIP-tile structure, which means that the random load presented in Figure 6, can lead to the same kind of failures at the same frequency 80Hz.

The dependence of the maximum amplitudes of self-induced vibrations on the frequency is given now by the equation following from (100):

$$C^2 = D_1 \omega^2 + D_2, \quad 0 \leq \omega \leq 500 \frac{1}{\text{sec}} \quad (104)$$

where

$$D_1 = 0.2 \cdot 10^{-8} \text{ sec}^2, \quad D_2 = -0.9 \cdot 10^{-5}$$

9. Conclusions. The following are the conclusions of this investigation:

1. A mathematical model describing parametrically excited torsional SIP-tile vibration has been developed. In the simplest case it is described by the second order non-linear differential equation with a periodical coefficients.
2. Applying the method of equivalent linearization the boundaries of parametrical instability have been defined.
3. Because of the non-linear properties of the SIP-tile model the amplitudes of torsional vibrations grow not without limit but up to a certain level of stable self-induced vibrations. This level depends on the exciting frequency. The maximum amplitude of self-induced vibrations corresponds to the frequency 80 Hz, where the relative amplitude of torsional vibrations is around 0.03. This amplitude  $C$  decreases with decrease of the exciting frequency  $\omega$  in the proportion:

$$\frac{C}{C_{max}} = \frac{\omega^2 - 4k_1 + 2q_0}{4q_0}$$

4. The equivalent torsion modulus  $G_{ttt}$  identified from experimental response data

$$G_{ttt} = 0.06 \text{ psi}$$

is very low which indicates that the SIP material works in the course of self-induced vibrations beyond the limits of stability of the shape of its filaments.

5. There are two ways to eliminate parametric resonances: a) shift the SIP-tile eigen-frequencies from the zone of parametrical resonance by changing the SIP-tile parameters, b) create a mechanism of a dissipation of energy in the course of self-induced vibrations.

The first way seems to be difficult to achieve because of a wide zone of resonance frequency (see the formula (63)).

The second way shows more promise: in order to depress the parametric resonance the damping coefficient  $\beta$  must be:

$$\beta > \frac{\pi q_0}{\omega}$$

or for the main resonance frequency 80 Hz the area of the loop of hysteresis of the SIP stress-strain characteristic must be:

$$S > 1.4 \text{ psi}$$

6. The analysis of self-induced vibration parametrically excited by random loads (Fig. 6) leads to the following results:

The unstable frequencies are in the domain:

$$0 \leq \omega \leq 45 \text{ Hz} \quad (C=0)$$

i.e. they are shifted toward the lower frequencies in comparison to the case of a single-harmonic excitation.

However, in contrast to the case of a single harmonic excitation the higher frequencies up to 80Hz also must be taken into account, because the instability at these frequencies occurs when initial torsional disturbances exceed some finite level while such disturbances can be generated because of instability at the lower frequencies.

Hence, the maximum amplitude of self-induced vibrations occurs at the frequency 80Hz and equals to 0.026.

This means that the behavior of the SIP-tile system under the random load given in Fig. 6 will be similar to its behavior in the course of the experiment mentioned above.

# REFERENCES

1. Zak, M., "Surface Phenomena in Elasticity" Journal of Elasticity, April, 1981.
2. Vulfson, Dynamics Analysis Cycle Mechanics, 1976, Leningrad (in Russian).